Memory erasure using time-multiplexed potentials

Saurav Talukdar, Shreyas Bhaban, and Murti V. Salapaka
University of Minnesota, Minneapolis, Minnesota 55455, USA

(Received 14 September 2016; revised manuscript received 22 May 2017; published 19 June 2017)

We study the thermodynamics of a Brownian particle under the influence of a time-multiplexed harmonic potential of finite width. The memory storage mechanism and the erasure protocol based on time-multiplexed potentials are utilized to experimentally realize erasure with work performed close to Landauer's bound. We quantify the work performed on the system with respect to the duty ratio of time multiplexing, which also provides a handle for approaching reversible erasures. A Langevin dynamics based simulation model is developed for the proposed memory bit and the erasure protocol, which guides the experimental realization. The study also provides insight into transport on the microscale.

DOI: 10.1103/PhysRevE.95.062121

I. INTRODUCTION

Landauer's principle, pioneered by Landauer in 1961, provides a critical link between information theory and thermodynamics of physical systems [1]. It states that there is no process where the work performed to erase one bit of information is less than k_bT ln 2 (Landauer's bound) when the prior probability of the bit being in any of the two states is equal [2]. Here, k_b is the Boltzmann constant, and T is the temperature of the heat bath.

Numerous analyses have corroborated Landauer's bound through different approaches [3–7]. The experimental study of Landauer's bound has only recently become viable, enabled by tools that provide access to processes with energetics on the scale of k_bT. The first such study in Ref. [8] examined Landauer's bound by employing optical traps to realize a single bit memory. Jun *et al.* [9] and Gavrilov and Bechhoefer [10] used an anti-Brownian electrokinetic feedback trap, and Hong *et al.* [11] used nanomagnetic memory bits to study Landauer's bound.

In this article, we study the stochastic energetics of transport realized by time multiplexing a harmonic potential of finite width to realize a bistable potential. Here a single laser in an optical tweezer setup is multiplexed between two locations with varying dwell times to create potentials (symmetric as well as asymmetric bistable potentials), that effectuate the erasure process. Furthermore, experimental variables for realizing reversible erasure are identified and utilized for approaching Landauer's bound. Langevin dynamics based simulations of a Brownian particle under the influence of a time-multiplexed laser is developed and is shown to obey quantitative trends observed in experiments. We use our method for shaping the potential by changing the dwell time of multiplexing of the laser to erase one bit of information. The ease of implementation and the high-resolution accounting of energetics are advantages of the method reported. We resort to the framework of stochastic energetics [12–15] to quantify the work performed on the system for the erasure process. The underlying principles developed in this article are applicable toward the study of transport achieved by time multiplexing of a single potential where realizations based on optical traps can be considered a particular instantiation of the general underpinnings of the framework presented.

II. MODEL FOR A ONE-BIT MEMORY

We use the abstraction of a Brownian particle in a double well potential to model a one-bit memory. The memory is designated state "zero" if the particle is in the left well and state one if it is in the right well. Experimentally, we realize a Brownian particle in a harmonic potential, albeit of finite width, by using a custom built optical tweezer setup to trap (near the focus of the objective lens) a polystyrene bead (1 μm in diameter) while suspended in deionized water. The bead represents the thermodynamic system of interest with the surrounding medium acting as a heat bath.

A. Bead in a laser trap

A laser passing through a high numerical aperture objective lens and incident on a bead in a solution traps the bead. Here, the bead experiences a harmonic potential with the equilibrium point (trap center) located near the focus of the lens. For small displacements away from the center of the trap, the bead experiences a restoring force directed towards the trap center [16,17]; the trap behaves like a Hookean spring with the restoring force being $k\,\Delta x$, where k is the stiffness of the trap and Δx is the distance between the bead center and the trap center. The position of the bead (denoted by x) is measured using a photodiode for a duration much larger than the time constant of the dynamics of the bead in the laser trap ($\sim$1 ms). The equilibrium probability distribution $P(x)$ of the position of the bead then is obtained by binning the measured position data. The potential energy landscape $U(x)$ of the bead in thermal equilibrium with the trap is obtained using the relation $U(x) = -\ln(\frac{P(x)}{C})$, where C is the normalization constant. In Fig. 1, the potential energy landscape experienced by an optical bead in a laser trap is shown (red and black curves), which is constant outside a distance w from the minimum of the potential and harmonic within the distance w from the equilibrium point.

The potential energy $U(x)$ is modeled by

$$U(x) = \begin{cases} \frac{1}{2}kx^2 + U_r, & \text{if } |x| \leqslant w, \\ \frac{1}{2}kw^2 + U_r, & \text{if } |x| > w, \end{cases} \tag{1}$$

which is harmonic up until a distance w (determined empirically from Fig. 1) from the stable equilibrium point. The stiffness k of the optical trap is determined experimentally by

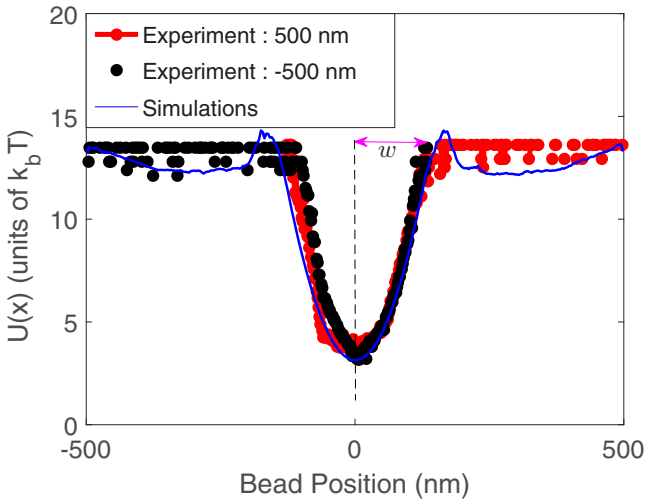

FIG. 1. The potential energy landscape of a bead in a laser trap. The experiments are performed with the bead initially at 500 nm (red curve) and −500 nm (black curve). The position of the bead is measured for 50 s. The potential $U(x)$ is mostly flat after a certain distance w from the stable equilibrium point. In the Monte Carlo simulations, the bead is initialized randomly between 500 and −500 nm. The position trajectory of the bead obtained from 100 Monte Carlo simulations is collected to determine $U(x)$ from simulations (blue curve).

applying the equipartition theorem, that yields $k = k_bT/\langle x^2\rangle$ [18]. The dynamics of the bead in a trap is modeled by the overdamped Langevin equation [15],

$$-\gamma\frac{dx}{dt} + \xi(t) - \frac{\partial U(x)}{\partial x} = 0, \tag{2}$$

where γ is the coefficient of viscosity (determined experimentally by the step response method [17]), $U(x)$ is the potential realized by the trap, and $\xi(t)$ is a zero mean uncorrelated Gaussian noise force. Here, $\langle\xi(t)\rangle = 0$, $\langle\xi(t),\xi(t')\rangle = 2D\delta(t-t')$ with the diffusion coefficient $D = \gamma k_bT$. The potential $U(x)$ described by (1) is used in conjunction with (2) to obtain 100 realizations (of 20 s each) of the bead trajectories. These realizations are, in turn, used to reconstruct the potential felt by the bead by binning the position trajectories. A close match with experimental results is seen as shown in Fig. 1.

B. Double well potential model of memory

A double well potential with two locally stable equilibrium points located at L and $-L$ is created by alternately focusing the trapping laser between the two locations by time multiplexing using an acousto-optical deflector. The laser is multiplexed at least 100 times faster than the time constant of the dynamics of the bead. The trapping laser multiplexed at the two locations is the external agent coupled to the thermodynamic system of interest formed by the bead. We define duty-ratio d as the fraction of the total time period the laser spends at location $-L$. The nature of the effective potential experienced by the Brownian particle can be manipulated by adjusting the duty ratio. The potential energy landscape $U(x,d)$, experienced by the bead for a duty-ratio d, is determined by the relationship $P_d(x) = Ce^{-U(x,d)/k_bT}$, where $P_d(x)$ is determined by binning

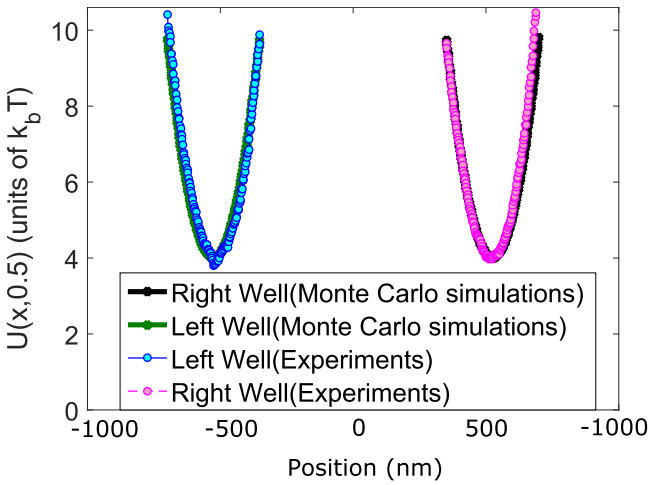

FIG. 2. Double well potential for $L = 550$ nm obtained using Monte Carlo simulations and experiments.

the measured position of the bead. Maintaining a duty ratio of 0.5 results in near identical parabolic potential wells at L and $-L$ as shown in Fig. 2, whereas a duty ratio greater than 0.5 leads to asymmetric double well potentials as shown in Fig. 3.

The bead dynamics under the influence of a time-multiplexed potential is modeled by the following Langevin equation:

$$-\gamma\frac{dx}{dt} + \xi(t) - \frac{\partial U(x,d)}{\partial x} = 0, \tag{3}$$

where the model for the potential $U(x,d)$ used in (3) incorporates the experimental observation that, for the duration when the laser remains focused at location L or $-L$, the bead experiences a harmonic potential up until a distance w from the trap focus. However, beyond the distance w from the locally stable equilibrium points L or $-L$, the bead undergoes a random walk [19]. Based on these observations, the potential $U(x,d)$ is modeled by

$$U(x,d) = \begin{cases} \frac{1}{2}k(x-L)^2 + U_r, & \text{if } |x-L| \leqslant w,\ r(t) = 1, \\ \frac{1}{2}k(x+L)^2 + U_r, & \text{if } |x+L| \leqslant w,\ r(t) = 0, \\ \frac{1}{2}kw^2 + U_r, & \text{otherwise,} \end{cases} \tag{4}$$

where $r(t)$ denotes the binary variable representing the presence or absence status of the laser at L. If the laser is focused at L, then $r(t) = 1$, otherwise $r(t) = 0$. The stiffness of the laser trap k and the width of the corresponding parabolic potential w are determined by characterization of the finite width harmonic potential obtained due to a single trap as described earlier in (1). The laser is multiplexed between the two locations at a significantly faster rate (∼10 μs) than the time constant of the bead dynamics (∼1 μs), which supports the model in (4). Monte Carlo simulations performed using (3) and the subsequent potential $U(x,d)$ reconstructed from bead position data (using the canonical distribution) yield potentials that match closely with experimental observations as seen in Fig. 2. We remark that, in the Monte Carlo simulations as well as in experiments, the stiffness of each of the wells formed at

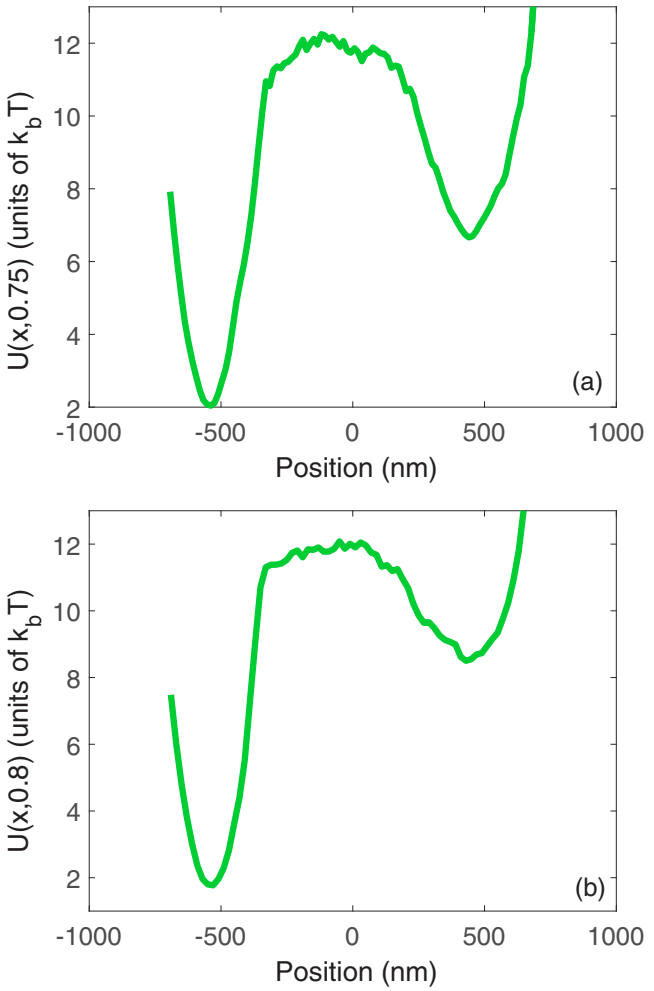

FIG. 3. The effect of the duty ratio on the nature of the double well potential. Increasing the duty ratio at $-L$ from 0.75 in (a) to 0.8 in (b), increases the asymmetry of the potential.

L and $-L$ when the duty ratio is 0.5 is close to $\frac{k}{2}$, which is half the stiffness of the single trap. To summarize, the model parameters (k and w) determined for a single trap are used in the Monte Carlo simulations of the bead in a double well potential realized by time multiplexing of the trapping laser. A close match between simulation and experimental results is observed as shown in Fig. 2. Using the Brownian particle in a double well potential model of a single bit memory, we next present an erasure protocol based on multiplexing of potentials.

III. ERASURE PROCESS

Erasure is a logically irreversible operation [20] where, irrespective of the initial state of the memory, the final state is zero (also known as the "reset-to-zero" operation). A bead in a double well potential is used to model a single-bit memory. No prior information on the state of the memory is assumed initially; thus, it is equally likely that the memory assumes state zero or one. However, at the end of the erasure process the memory state is *zero* (the bead must be in the left well). Thus, there is no change in the average energy of the bead in an erasure process (as the depth of both wells is the same), whereas the decrease in entropy associated with erasure is $k_b \ln 2$; thereby requiring at least a $k_bT \ln 2$ amount of work to be performed on the system [2]. We note that Landauer's bound is applicable to the average work performed on the system over many realizations of the bead trajectory, but, it is possible to obtain individual erasure realizations with the work performed on the system less than $k_bT \ln 2$. Indeed we demonstrate later that, for a fraction of trajectories, the work performed on the bead is lower than $k_bT \ln 2$ (see Fig. 6).

Landauer's bound of $k_bT \ln 2$ holds if the erasure process is always successful. It can be shown that, for imperfect erasure schemes with the probability of successful erasure being p, at least a $k_bT[\ln 2 + p \ln p + (1-p)\ln(1-p)]$ amount of work is required to be performed on the system [2]. It is important to note that the bound decays rapidly as p decreases from 1 with the bound being $k_bT \ln 2$ for $p = 1$ and zero for $p = 0.5$. In our paper, we ensure that $p > 0.95$ and assume that the erasure process is always successful.

The erasure protocol is described next where the duty ratio is the fraction of the time spent by the laser at location $-L$ [see Fig. 4(c)] as compared to L; the higher the duty ratio, the more the time spent by the laser at $-L$. In the first phase of the protocol, the memory model of a Brownian particle in a symmetric double well potential is obtained by maintaining a duty ratio of 0.5 for a duration of 10 s. Next, in the second phase of the protocol, an asymmetric well is realized with the well at $-L$ deeper than the well at L, which is obtained by maintaining the duty ratio to be greater than 0.5 for a duration (dependent on the choice of d) of τ s. Finally, we revert the duty ratio to a value of 0.5 to complete the reset-to-zero process (for a duration of 10 s). The success of erasing the memory depends on the magnitude of the deviation of the duty ratio from 0.5 and the time duration τ during the second phase.

In the second phase, over the time duration τ, the laser spends more time focused at $-L$ than at L, enabling an asymmetric potential landscape as is observed in Fig. 3. Increasing the duty ratio results in a lower barrier height for the right to the left transition than for the left to the right transition. It thus favors the transport of the bead from the right to the left well if the bead is initially in the right well as shown in Fig. 4(a) and retains the bead in the left well if it was initially in the left well as shown in Fig. 4(b). The duration τ is chosen to be a few multiples of the average exit time of the bead from the right well but less than the average exit time of the bead from the left well, which ensures a high likelihood of the bead's final location to be in the left well. For example, we choose τ as 30 s for the duty ratio of 0.7, which is approximately three times the observed exit time of the bead from the right well.

The above mentioned erasure mechanism ensures a high success proportion as reported in Fig. 5. It is seen that the duty ratio of 0.65 yields a success proportion significantly less than 0.95, whereas a duty ratio of >0.7 shows a success proportion greater than 0.95. Similar trends are reflected from Monte Carlo simulations as well as experiments as seen in Fig. 5. Thus, to ensure a high success proportion in order to demonstrate erasures with energy expenditures close to Landauer's bound, we operate our erasure protocol at a duty ratio of at least 0.7. In the next section, we quantify the work performed on the bead in an erasure process for a given duty ratio.

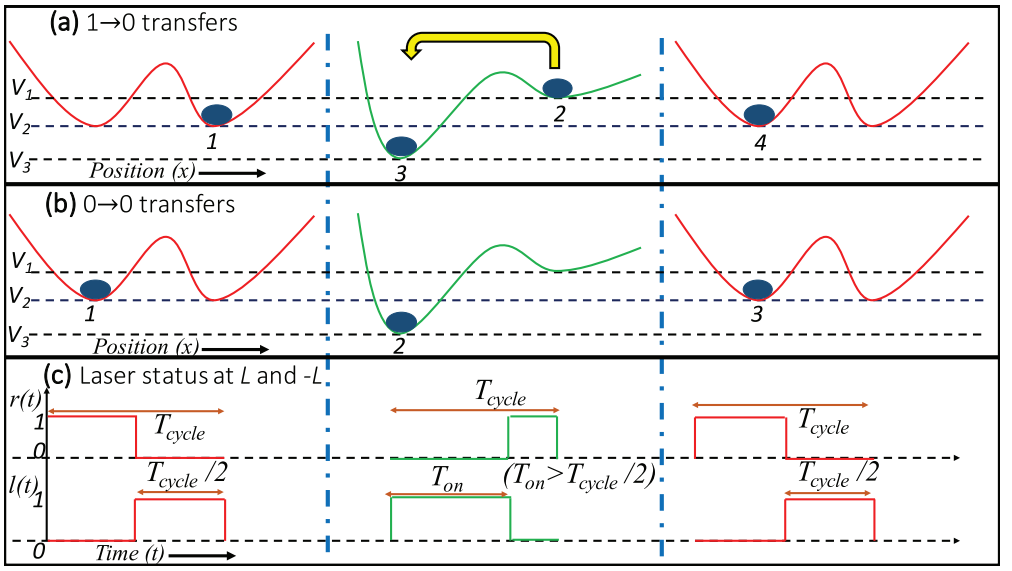

FIG. 4. (a) A schematic showing the erasure process with a bead initially in the right well. The initial bead position is 1 (right well) with potential energy V_2. The duty-ratio d in the left well then is increased, which lifts the bead and takes it to position 2 with energy V_1. Thermal fluctuations enable the bead to cross the barrier and reach position 3 with energy V_3. Decreasing the duty ratio back to 0.5 lifts the bead to position 4, which has energy V_2. The process $1 \to 2 \to 3 \to 4$ is the erasure process. (b) A schematic showing the erasure process with a bead initially in the left well. Here, the process $1 \to 2 \to 3$ is the erasure process. (c) The signals $r(t)$ and $l(t)$ denote the presence or absence status of the laser at L and $-L$, respectively. A value of 1 means present, and 0 means absent. To ensure a duty ratio greater than 0.5, we maintain $d = T_{\text{on}}/T_{\text{cycle}} > 0.5$.

IV. ERASURE THERMODYNAMICS

We now utilize the stochastic-energetics framework for the Langevin systems [14,15] and quantify the work performed on the system associated with the erasure process realized by manipulation of the duty ratios. The external system does work on the bead by changing the duty ratio, which results in modifying the potential felt by the bead. For an erasure process, the work performed on the bead dW is given by

$$dW = \sum_j \{U[x(t_j), d(t_j^+)] - U[x(t_j), d(t_j^-)]\}, \tag{5}$$

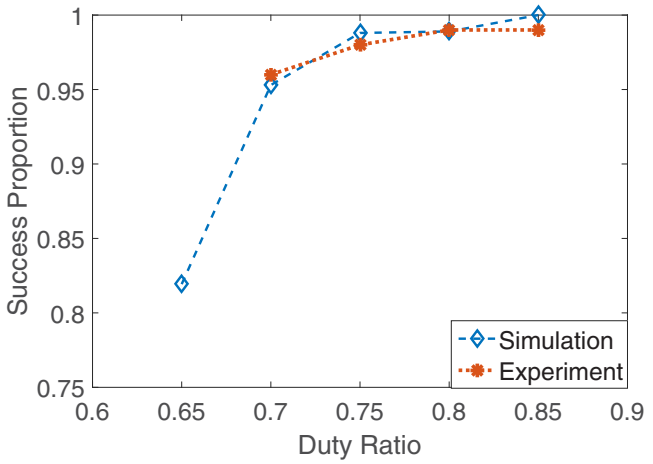

FIG. 5. Effect of the duty ratio on success proportion p. The duty ratio of 0.65 has a success proportion of 0.82, whereas, a duty ratio greater than 0.7 yields a success proportion higher than 0.95.

where d denotes the discontinuous parameter (here, the duty ratio) changed by the external system and t_j denotes the time instances when the parameter was changed (t_j^- and t_j^+, respectively, denote the instants just before and after changing the parameter).

Landauer's bound can be reached when the erasure process is performed in a quasistatic manner. For an erasure performed over a large but finite duration τ, the average work performed on the system is [13] as follows:

$$\langle dW \rangle = dW_{\text{Landauer}} + \frac{B}{\tau}, \tag{6}$$

where $dW_{\text{Landauer}} = k_b T \ln 2 = 0.693 k_b T$. The duration for which an asymmetric double well potential is realized τ is chosen to be a multiple of the exit time τ_e of the bead from the right well. It is known that $\tau_e \propto \frac{\exp(\delta U_r)}{\sqrt{k_r}}$ [21], where δU_r is the barrier height of the right well, k_r is the stiffness of the right well, and $\exp(\cdot)$ is the exponential function. Note that $d - 0.5$ is indicative of the asymmetric nature of the double well potential; the higher the value, the more the asymmetry. We determine the dependency of δU_r and k_r on $\frac{1}{d-0.5}$ empirically. The dependency of normalized δU_r and k_r on $\frac{1}{d-0.5}$ is shown in Figs. 6 and 7, respectively. It follows that $\tau \propto \tau_e \propto \frac{\exp\left(\frac{0.99}{d-0.5}\right)}{\sqrt{\frac{1}{d-0.5}}}$. Substituting it in (6) for τ leads to

$$\langle dW \rangle = dW_{\text{Landauer}} + B\frac{\exp\left(-\frac{0.99}{d-0.5}\right)}{\sqrt{d-0.5}}. \tag{7}$$

Reducing d, the time duration τ required for successful erasures increases, whereby the erasure process approaches a quasistatic process. Thus, the duty ratio provides a handle for

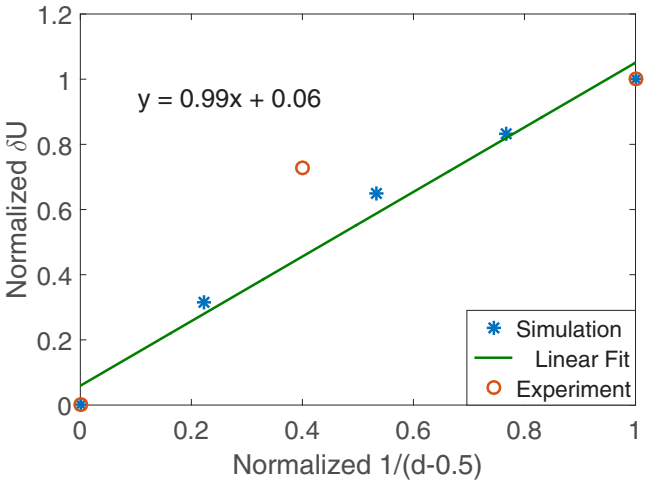

FIG. 6. The blue and red points represent the normalized barrier heights of the right well as a function of $\frac{1}{d-0.5}$, obtained using simulations and experiments, respectively. The green line is the least squares fit to the simulation data points.

realizing quasistatic erasure processes using time-multiplexed potentials.

The average work performed on the bead $\langle dW \rangle$ for duty-ratio $d > 0.7$ obtained using simulations and experiments is shown in Figs. 8 and 9, respectively. For a duty ratio of 0.7, the average work performed on the system obtained from Monte Carlo simulations is $0.73 \pm 0.037 k_b T$, whereas experimentally for a duty ratio of 0.7, the average work performed on the bead is obtained to be $0.9 \pm 0.106 k_b T$. The average work of $0.9 \pm 0.106 k_b T$ to erase a bit of information is the closest to Landauer's bound of $k_b T$ ln 2 reported. As the duty ratio is reduced [$1/(d - 0.5)$ increased], the average work performed on the bead decreases as observed in the simulations as well as experiments.

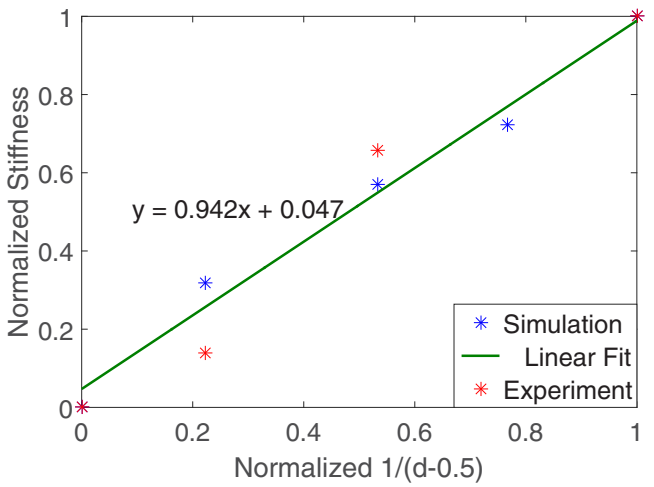

FIG. 7. The blue and red points represent the normalized stiffnesses of the right well as a function of $\frac{1}{d-0.5}$, obtained using simulations and experiments, respectively. The green line is the least squares fit to the simulation data points.

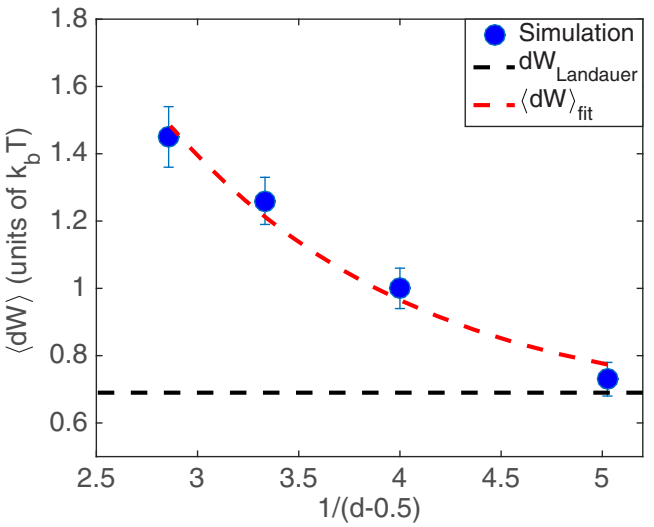

FIG. 8. The blue circles represent the average work performed on the bead obtained using 300 Monte Carlo realizations (150, $0 \rightarrow 0$ and 150, $1 \rightarrow 0$ transfers) for duty ratios of 0.7, 0.75, 0.8, and 0.85. The vertical lines represent the standard error in the mean for each duty ratio. The black dotted line denotes the Landauer bound of $k_b T$ ln 2. The red dotted line is the fit with the free parameters A and B.

We fit the model derived in (7) $\langle dW \rangle_{\text{fit}} = A + B \frac{\exp(-\frac{0.99}{d-0.5})}{\sqrt{d-0.5}}$ to the average work performed on the bead obtained by simulations and experiments for various duty-ratio values with A and B being free parameters (see Fig. 9). Using the simulation data we obtain $A = 0.65 k_b T$, $B = 8.49 k_b T$, whereas for the experimental data we have $A = 0.70 k_b T$, $B = 35.04 k_b T$. It is seen that A (which represents the average work

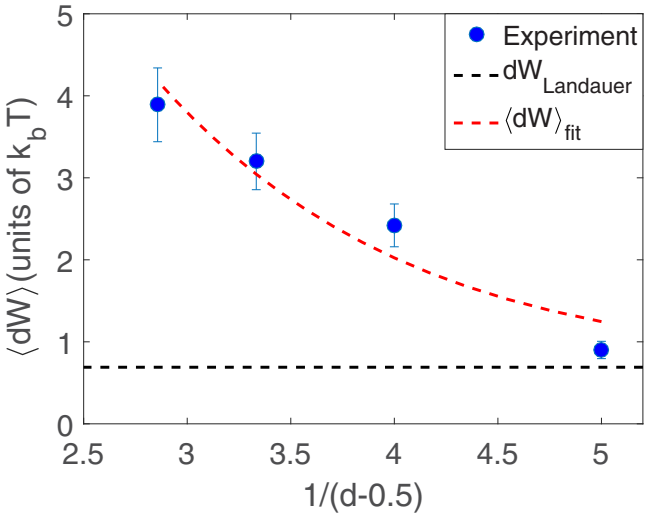

FIG. 9. The blue circles represent the average work performed on the bead obtained from 100 experiments (50, $0 \rightarrow 1$ and 50, $1 \rightarrow 1$ transfers) for duty ratios of 0.7, 0.75, 0.8, and 0.85. The vertical lines represent the standard error in the mean for each duty ratio. The black dotted line denotes the Landauer bound of 0.7, 0.75, 0.8, and 0.85. The red dotted line is the fit with the free parameters A and B.

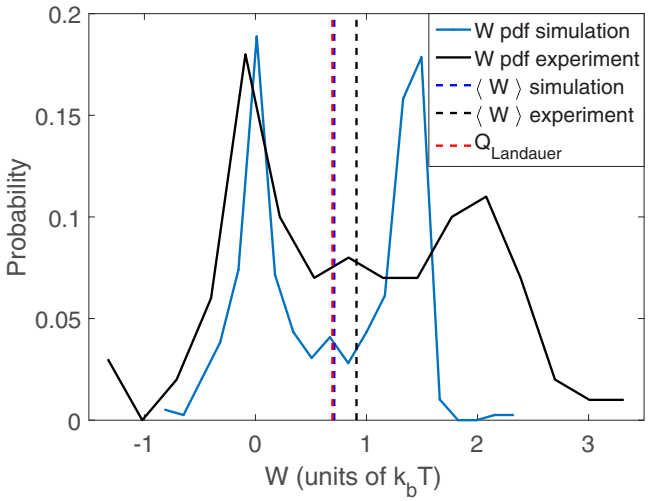

FIG. 10. The distribution of work performed on the bead obtained from the simulations and experiments for a duty ratio of 0.7. The nature of the distribution is bimodal.

performed on the system in the quasistatic case) has a value close to the Landauer bound of k_bT ln 2 ($= 0.693k_bT$) in both simulations as well as experiments.

The distribution of work performed while erasing a bit at a duty ratio of 0.7, obtained from simulations and experiments, is shown in Fig. 10. It is evident that for a fraction of trajectories, the work performed on the bead is less than Landauer's bound; indeed, for some trajectories it is negative. However, the mean of the distribution is close to Landauer's bound. Moreover, a bimodal nature of the distribution is evident. The mode on the right in Fig. 10 corresponds to work performed on the particle for the transition from the right to the left well (or $1 \rightarrow 0$), and the mode on the left corresponds to the transition from the left to the left well (or $0 \rightarrow 0$). The characteristics of the simulation data are confirmed by experiments as shown in Fig. 10. On increasing the duty ratio, the mode on the right shifts further to the right as the work performed on the bead is higher for higher duty ratios. This results in an increase in the standard error in the mean on increasing the duty ratio as shown by the length of the blue bars in Figs. 8 and 9.

Thus we have demonstrated that a single-bit memory and its associated erasure protocol can be realized by multiplexing a laser between two locations. The resulting energetics can effectively be accounted for in the framework developed by Sekimoto [12–15], and the magnitude of the deviation of the duty ratio of multiplexing from 0.5 provides an effective means for driving the erasure process toward a quasistatic process.

Error quantification

The primary sources of errors in the average work performed on the system computed from position measurements are introduced by the photodiode based measurements. The error statistics of the photodiode used in the experiments are quantified in Ref. [22] and are shown to have a zero mean and a standard deviation on the order of a nanometer. Assuming that the error in position measurement e_x is independent of the actual bead position x, the average error in the potential energy of the bead e_U is given by

$$\begin{aligned}\langle e_U \rangle &= \left\langle \tfrac{1}{2}k(x + e_x - L)^2 - \tfrac{1}{2}k(x - L)^2 \right\rangle \\ &= \tfrac{1}{2}k\langle e_x^2 \rangle \sim 10^{-3}k_bT.\end{aligned}$$

Thus, the error in obtaining the work performed on the bead in a realization of erasure is on the order of $10^{-3}k_bT$.

V. CONCLUSIONS

In this article, we study the thermodynamics of a Brownian particle influenced by the time multiplexing of a single harmonic potential of finite width. A Monte Carlo simulation framework for a Brownian particle under the influence of a time-multiplexed laser also is developed and shown to obey qualitative trends observed in experiments. We demonstrate that the duty ratio provides a handle on the speed of the erasure process and its approach to reversibility. It is established through experiments and simulations that reducing the duty ratio results in the erasure process with the average work performed approaching k_bT ln 2; which is the minimum average work required to erase one bit of information. Furthermore, the method is easy to implement on a standard optical tweezer setup. The insight obtained from this article can potentially be leveraged to realize practical devices that yield erasure mechanisms with energetics on the order of k_bT ln 2.

ACKNOWLEDGMENTS

We would like to thank Prof. A. Majumdar, Stanford University for initial discussion about the problem, Prof. S. Salapaka, University of Illinois, Urbana Champaign for his comments, T. Aggarwal, Cymer LLC, S. Roychowdhury, GE Research for their contributions towards building the optical tweezer setup. The research reported was supported by the National Science Foundation under Grant No. CMMI-1462862.

S.T. and S.B. contributed equally to this work. S.T., S.B., and M.V.S. conceptualized the work. S.T. and S.B. developed the computational framework and conducted experiments.

[1] R. Landauer, IBM J. Res. Dev. **5**, 183 (1961).
[2] J. M. Parrondo, J. M. Horowitz, and T. Sagawa, Nat. Phys. **11**, 131 (2015).
[3] K. Shizume, Phys. Rev. E **52**, 3495 (1995).
[4] R. Dillenschneider and E. Lutz, Phys. Rev. Lett. **102**, 210601 (2009).
[5] B. Lambson, D. Carlton, and J. Bokor, Phys. Rev. Lett. **107**, 010604 (2011).
[6] B. Piechocinska, Phys. Rev. A **61**, 062314 (2000).
[7] T. Sagawa and M. Ueda, Phys. Rev. Lett. **102**, 250602 (2009).
[8] A. Bérut, A. Arakelyan, A. Petrosyan, S. Ciliberto, R. Dillenschneider, and E. Lutz, Nature (London) **483**, 187 (2012).
[9] Y. Jun, M. Gavrilov, and J. Bechhoefer, Phys. Rev. Lett. **113**, 190601 (2014).
[10] M. Gavrilov and J. Bechhoefer, Phys. Rev. Lett. **117**, 200601 (2016).

[11] J. Hong, B. Lambson, S. Dhuey, and J. Bokor, Sci. Adv. **2**, e1501492 (2016).
[12] K. Sekimoto, J. Phys. Soc. Jpn. **66**, 1234 (1997).
[13] K. Sekimoto and S. Sasa, J. Phys. Soc. Jpn. **66**, 3326 (1997).
[14] K. Sekimoto, Prog. Theor. Phys. Suppl. **130**, 17 (1998).
[15] K. Sekimoto, *Stochastic Energetics* (Springer, Berlin, 2010), Vol. 799.
[16] A. Ashkin, J. Dziedzic, J. Bjorkholm, and S. Chu, Opt. Lett. **11**, 288 (1986).
[17] K. Visscher and S. M. Block, Methods Enzymol. **298**, 460 (1998).
[18] K. C. Neuman and S. M. Block, Rev. Sci. Instrum. **75**, 2787 (2004).
[19] S. Bhaban, S. Talukdar, and M. Salapaka, 2016 American Control Conference (ACC) (IEEE, Piscataway, NJ, 2016), pp. 5823–5829.
[20] C. H. Bennett, Int. J. Theor. Phys. **21**, 905 (1982).
[21] C. W. Gardiner *et al.*, *Handbook of Stochastic Methods* (Springer, Berlin, 1985), Vol. 4.
[22] T. Aggarwal and M. Salapaka, Rev. Sci. Instrum. **81**, 123105 (2010).